Journal of Ceramic Processing Research. Vol. 11, No. 5, pp. 617~621 (2010)

J O U R N A L O F
Ceramic Processing Research

Mechanical synthesis and rapid consolidation of a nanostructured Cu-ZrO_2 composite by high frequency induction heating

In-Jin Shon[a,b], In-Yong Ko[a,*], Seung-Myoung Chae[a], Hyun-Su Kang[a], Jung-Mann Doh[c] and Kyung-Tae Hong[c]

[a]*Division of Advanced Materials Engineering and the Research Center of Industrial Technology, Engineering College, Chonbuk National University, 561-756, Republic of Korea*

[b]*Department of Hydrogen and Fuel Cells Engineering, Specialized Graduate School, Chonbuk National University, 561-756, Republic of Korea*

[c]*Advanced Functional Materials Research Center, Korea Institute of Science and Technology, PO Box 131, Cheongryang, Seoul 130-650, Republic of Korea*

Nanopowders of Cu and ZrO_2 were synthesized from 2CuO and Zr by high energy ball milling. The powder sizes of Cu and ZrO_2 were 20 nm and 30nm, respectively. A dense nanocrystalline 2Cu-ZrO_2 composite was consolidated by a high frequency induction heated sintering method within 1 minute from the mechanically synthesized powders(2Cu-ZrO_2) and horizontally milled 2CuO+Zr powders. The average hardness and fracture toughness values of nanostuctured 2Cu-ZrO_2 composite were investigated.

Key words: High frequency induction heated sintering, Composite, Nanomaterial, Mechanical properties, Cu-ZrO_2.

Introduction

It is well known that attractive physical and mechanical properties can be obtained with metal matrix composites, such as high specific modulus, strength-to weigh ratio, fatigue strength, and temperature stability and wear resistance, which have been documented extensively [1-5]. ZrO_2 has a density of 5.98 g cm^{-3}, a Young's modulus of 210 GPa, excellent oxidation resistance and good high-temperature mechanical properties [6, 7]. Cu has a density of 8.9 g cm^{-3}, a Young's modulus of 130 GPa and good fracture toughness [7]. Hence, a microstructure consisting of Cu and ZrO_2 may be able to satisfy the good oxidation resistance and high temperature mechanical property requirements of a successful high temperature structural material.

Traditionally, discontinuously reinforced metal matrix composites have been produced by several processing routes such as powder metallurgy, spray deposition mechanical alloying, various casting techniques and SHS(self-propagating high temperature synthesis). All these techniques are based on the addition of ceramic reinforcements to the matrix materials which may be in a molten or powder form. Of all these techniques, high energy ball milling and mechanical alloying of powder mixtures, were reported to be efficient techniques for the preparation of nano-crystalline metals and alloys, which is a combination of mechanical milling and chemical reactions [8].

*Corresponding author:
Tel : +82-63-270-2295
Fax: +82-63-270-2386
E-mail: plasma@chonbuk.ac.kr

Nanostructured materials have been widely investigated because they have a wide functional diversity and exhibit enhanced or different properties compared with bulk materials. Particularly, in the case of nanostructured ceramics, the presence of a large fraction of grain boundaries can lead to unusual or better mechanical, electrical, optical, sensing, magnetic, and biomedical properties [9-15]. In recent days, nanocrystalline powders have been developed by co-precipitation, a thermochemical and thermomechanical process named as the spray conversion process (SCP), and high energy milling [16, 17]. The grain size in sintered materials, however, becomes much larger than that in pre-sintered powders due to the fast grain growth during a conventional sintering process. Therefore, controlling grain growth during sintering is one of the keys to the commercial success of nanostructured materials. In this regard, the high frequency induction activated sintering method which can make dense materials within 2 minunites, has been shown to be effective in achieving this goal [18].

The purpose of this study is to produce nanopowders of Cu, ZrO_2 and dense nanocrystalline Cu-ZrO_2 composite within 1 minutes from mechanically synthesized powders (2Cu-ZrO_2) and horizontally milled 2CuO + Zr powders using this novel induced current activated sintering method and to evaluate its mechanical properties (hardness and fracture toughness).

Experimental Procedure

Powders of 99% CuO (< 5 μm, Aldrich, Inc) and 99.5% pure Zr(−325 mesh, Sejong, Inc) were used as starting

materials. 2CuO and Zr powders were mixed by two types of method. Firstly, the powders was milled in a high-energy ball mill, a Pulverisette-5 planetary mill at 250 rpm and for 10 h. Tungsten carbide balls (8.5 mm in diameter) were used in a sealed cylindrical stainless steel vial under an argon atmosphere. The weight ratio of balls-to-powder was 30 : 1. Secondly, the powders were mixed in polyethylene bottles using zirconia balls with ethanol and rotated at a horizontal rotation velocity of 250 rpm for 10 h. The grain sizes of Cu and ZrO_2 were calculated by Suryanarayana and Grant Norton's formula [19] :

$$B_r\ (B_{crystalline} + B_{strain})\ cos\theta = k\lambda/L + \eta sin\theta \quad (1)$$

where B_r is the full width at half-maximum (FWHM) of the diffraction peak after instrumental correction; $B_{crystalline}$ and B_{strain} are the FWHM caused by small grain size and internal stress, respectively; k is constant (with a value of 0.9); l is wavelength of the X-ray radiation; L and η are the grain size and internal strain, respectively; and θ is the Bragg angle. The parameters B and B_r follow Cauchy's form with the relationship: $B = B_r + B_s$, where B and B_s are the FWHM of the broadened Bragg peaks and a standard sample's Bragg peaks, respectively.

After milling, the mixed powders were placed in a WC die (outside diameter, 40 mm; inside diameter, 5 mm; height, 40 mm) and then introduced into the high frequency induction heated sintering system made by Eltek in South Korea shown schematically in Fig. 1. The four major stages in the synthesis are as follows. The system was evacuated (stage 1). And a uniaxial pressure of 500 MPa was applied (stage 2). An indued current was then activated and maintained to 630 °C with heating rate of 700 K·minute^{-1} and then turned off without a holding time (stage 3). The temperature was measured by a pyrometer focused on the surface of the graphite die. At the end of the process, the sample was cooled to room temperature (stage 4).

The relative densities of the synthesized sample were measured by the Archimedes method. Microstructural information was obtained from product samples which were polished. Compositional and microstructural analyses of the products were made through X-ray diffraction (XRD) and scanning electron microscopy (SEM) with energy dispersive X-ray analysis (EDAX). Vickers hardness was measured by performing indentations at a load of 20 kg and a dwell time of 15 s on the synthesized samples.

Results and Discussion

The interaction between 2CuO and Zr, i.e. :

$$2CuO + Zr \rightarrow 2Cu + ZrO_2 \quad (2)$$

is thermodynamically feasible as shown in Fig. 2 [20].

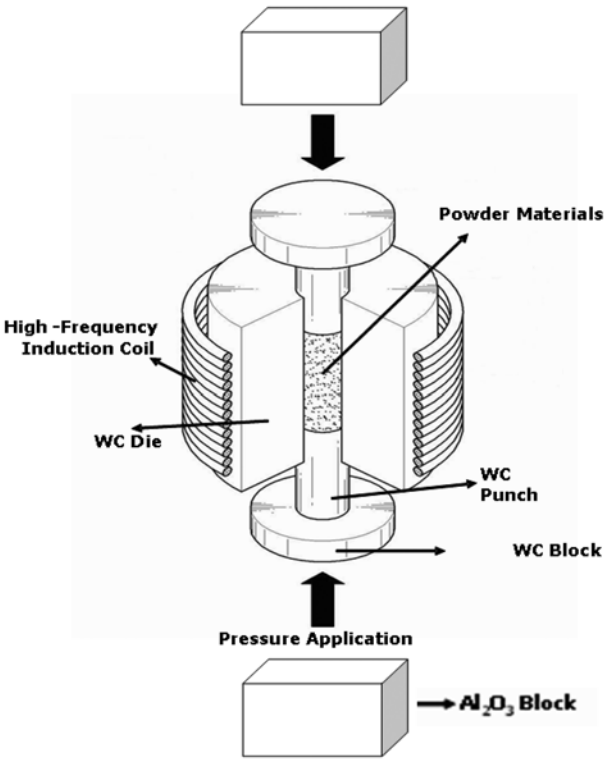

Fig. 1. Schematic diagram of the high frequency induction heated sintering apparatus.

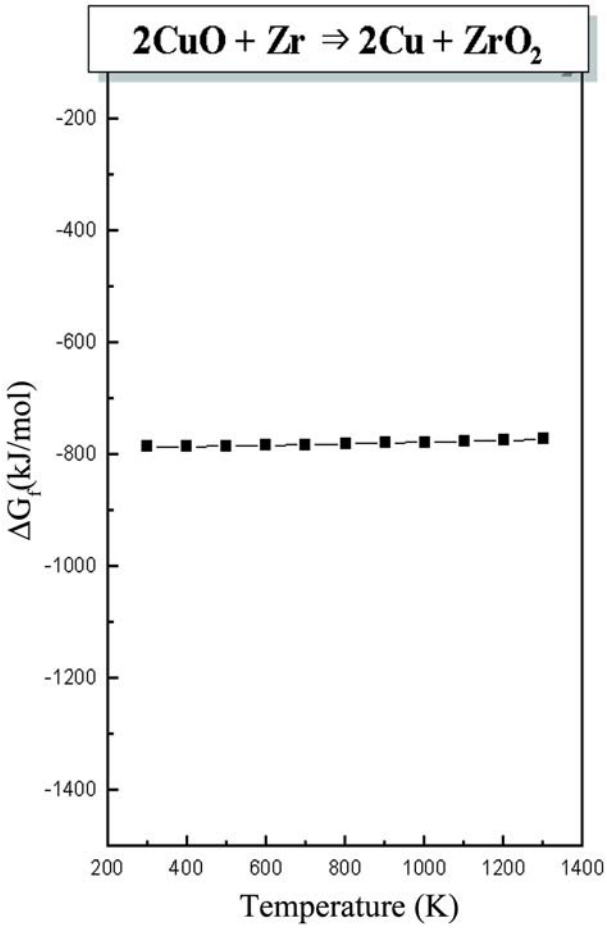

Fig. 2. Temperature dependence of the Gibbs free energy variation by interaction of 2CuO with Zr.

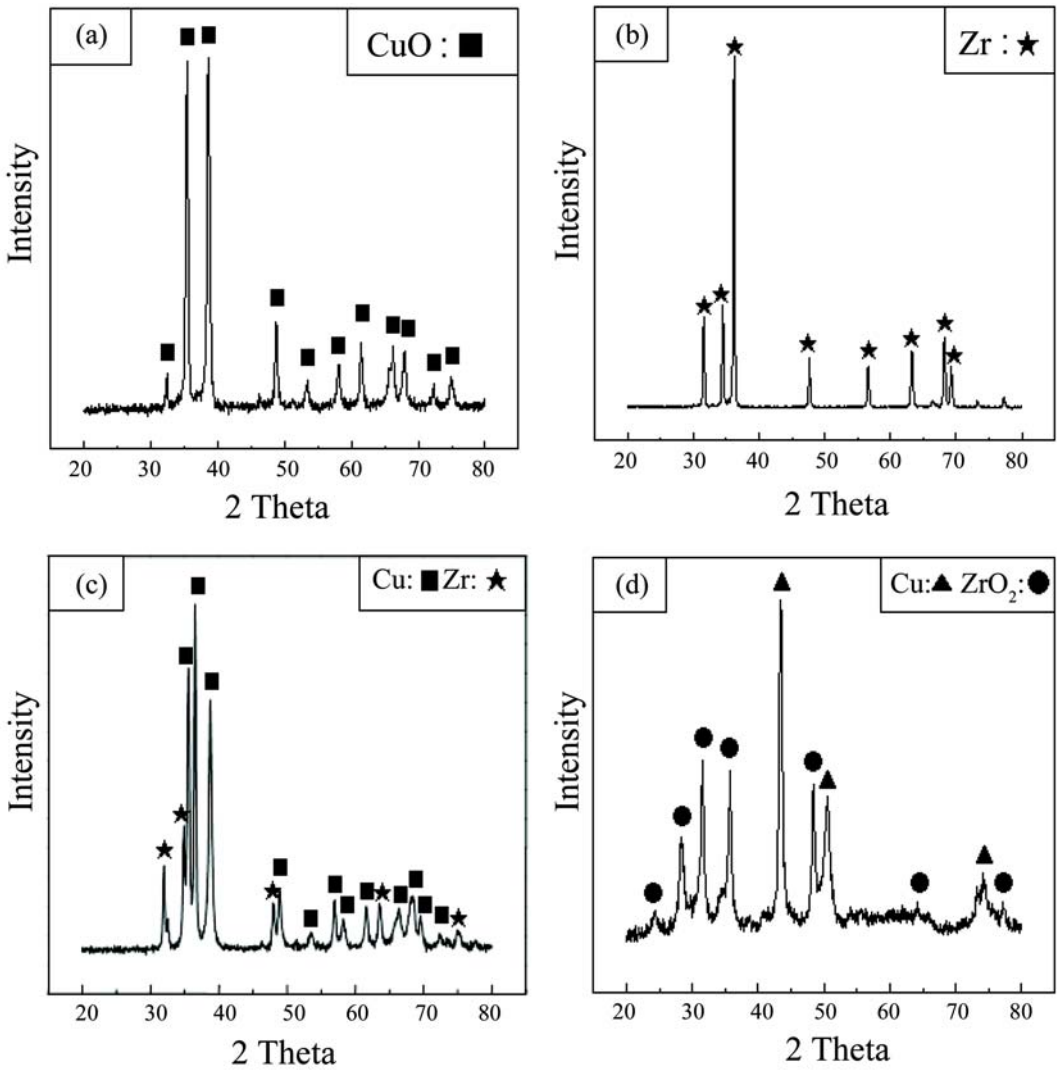

Fig. 3. XRD patterns of raw materials: (a) CuO, (b) Zr, (c) horizontally milled powders and (d) mechanically milled powders.

The X-ray diffraction patterns of horizontally milled powder and mechanically high energy ball milled powders from raw powders are shown in Fig. 3(c) and 3(d), respectively. Cu-ZrO_2 was not synthesized during the horizontal rotation ball milling in ethanol, but synthesized during high energy ball milling. From the above results, solid replacement reaction occurs completely during the high energy ball milling. The full width at half-maximum (FWHM) of the diffraction peak is broad due to refinement of the powder and strain. The average grain sizes of ZrO_2 and Cu measured by Suryanarayana and Grant Norton's formula were about 30 nm and 20 nm, respectively.

XRD patterns of the Cu-ZrO_2 composite heated to 630 °C are shown in Fig. 4. Only Cu and ZrO_2 peaks are detected. Fig. 5 shows plots of $B\cos\theta$ versus $\sin\theta$ to calculate the grain size of Cu and ZrO_2. The structural parameters, i.e. the average grain sizes of Cu and ZrO_2 in horizontal milling and high energy ball milling obtained from X-ray data in Fig. 5 by Suryanarayana and Grant Norton's formula, are 100, 53 nm and 92, 83 nm, respectively. And the relative

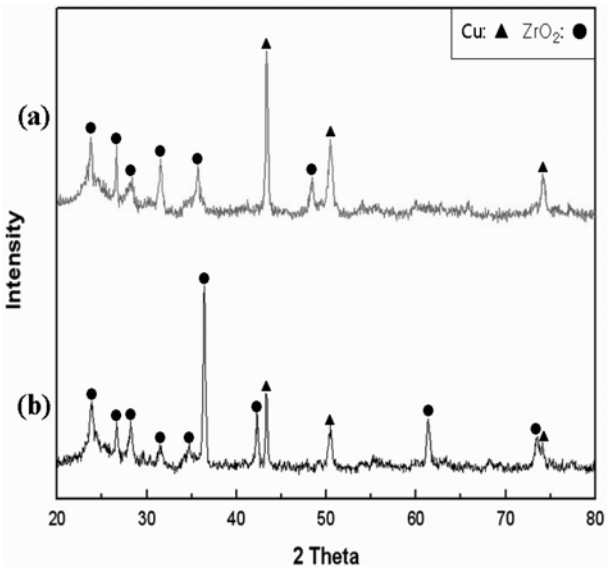

Fig. 4. XRD patterns of 2Cu-ZrO_2 composite sintered from (a) horizontally milled powders and (b) high energy ball milled powders.

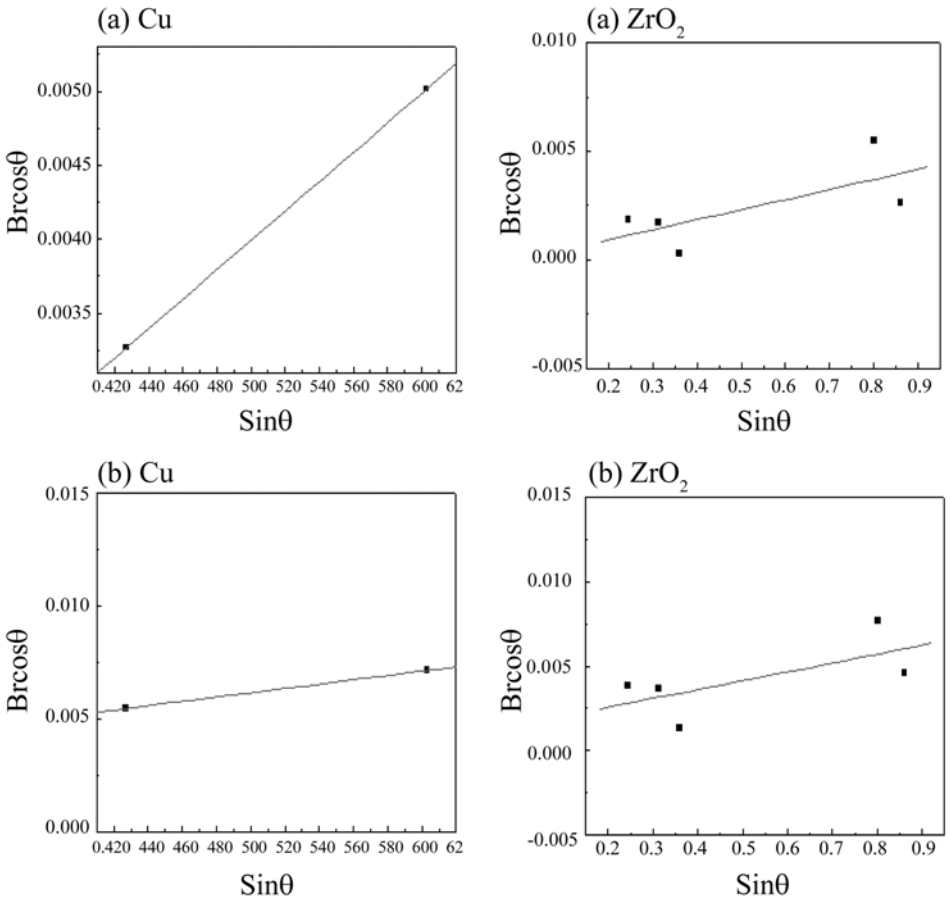

Fig. 5. Plot of Cu and ZrO_2 in 2Cu-ZrO_2 composite sintered from (a) horizontally milled powders and (b) high energy ball milled powders.

density of the Cu-ZrO_2 composites were 96% and 98%, respectively. FE-SEM images of Cu-ZrO_2 composite sintered at 630 ºC from horizontally milled powders and high energy ball milled powders are shown in Fig. 6. The composites consists of nanograins. It is considered that the reasons for the high density of the composite obtained at low temperature are as follows. Firstly, the application of pressure during the initial stage sintering adds another term to the surface energy driving force such that the total driving force, F_D, is now [21] :

$$F_D = \gamma + (P_a r/\pi), \quad (3)$$

where γ is the surface energy, P_a is the applied pressure, and r is the radius of the particle. The effect of pressure on the densification of nanometric, undoped zirconia during sinter-forging was investigated by Skandan *et al*. [22]. A significant increase in the relative density was observed as the pressure was increased from about 35 to 300 MPa for sintering at 950 ºC for 180 minutes. Secondly, the role of the current (resistive or inductive) in sintering and or synthesis has been the focus of several attempts aimed at providing an explanation of the observed enhancement of sintering and the improved characteristics of the products. The role played by the current has been variously interpreted, the effect being explained in terms of a fast heating rate due to Joule heating, the presence of a plasma in the pores

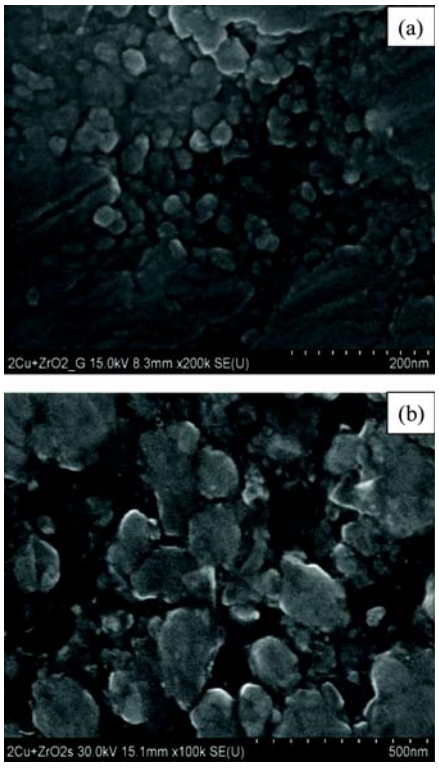

Fig. 6. FE-SEM images of 2Cu-ZrO_2 composite sintered from (a) high energy ball milled powders and (b) horizontally milled powders.

separating powder particles [23], and the intrinsic contribution of the current to mass transport [24-26].

Vickers hardness measurements were made on polished sections of the Cu-ZrO_2 composite using a 20 kg_f load and 15 s dwell time. The calculated hardness value of Cu-ZrO_2 composite sintered 630 °C from horizontally milled powders and high energy ball milled powders were 300, 330 kg/mm^2, respectively. This value represents an average of five measurements. Indentations with large enough loads produced median cracks around the indent. The length of these cracks permits an estimation of the fracture toughness of the material. From the length of these cracks, fracture toughness values can be determined using Anstis *et al*. [27] equeation :

$$K_{IC} = 0.016\ (E/H)^{1/2} \cdot P/C^{3/2} \quad (4)$$

where E is Young's modulus, H the indentation hardness, P the indentation load, and C the trace length of the crack measured from the center of the indentation. The modulus was estimated by the rule of mixtures for the 0.59 volume fraction of ZrO_2 and the 0.41 volume fraction of Cu using $E(ZrO_2) = 210$ GPa [6] and $E(Cu) = 130$ GPa [7]. As in the case of hardness values, the toughness values were derived from the average of five measurements. The toughness values of composites obtained from horizontally milled powders and high energy ball milled are 7 and 7.5 $MPa \cdot m^{1/2}$, respectively.

The hardness and fracture toughness of ZrO_2 are reported as 11.8 GPa and 6.5 $MPa \cdot m^{1/2}$, respectively [28]. The hardness of 2Cu-ZrO_2 composite is lower than that of monolithic ZrO_2 but the fracture toughness is higher than that of ZrO_2 due to the addition of ductile Cu.

Conclusions

Nanopowders of ZrO_2 and Cu were synthesized from Zr and 2CuO by high energy ball milling. The powder sizes of Cu and ZrO_2 were 20 nm and 30 nm, respectively. Using the high frequency induction heated sintering method (HFIHS), the densification of a nanostructured 2Cu-ZrO_2 composite was accomplished from mechanically synthesized powders and horizontally milled powders within the duration of 1 minute. The average grain sizes of Cu and ZrO_2 prepared by HFIHS were lower than 100 nm. The average hardness and fracture toughness values obtained from mechanically synthesized powders and horizontally milled powders were 330 and 300 kg/mm^2, and 7.5 and 7 $MPa \cdot m^{1/2}$, respectively. The fracture toughness of the 2Cu-ZrO_2 composite is higher than that of monolithic ZrO_2 .

Acknowledgment

"We are grateful for the financial support from the Korea Institute of Science and Technology, which was provided through the program for study on Development of Surface Treatment for Light Metals".

References

1. L. Ceschini, G. Minak and A.Morri, Composites Science and Technology 66 (2006) 333-342.
2. S.C. Tjong and Z.Y. Ma, Materials science and Engineering 29 (2000) 49-113.
3. D.J. Lloyd, Int Mater Rev. 39 (1994) 1-23.
4. J.M. Torralba and F. Velasco, J Mater Process Technol. 133 (2003) 203-205.
5. R. Fan, B. Liu, J. Zhang, J. Bi and Y. Yin, Mater. Chem. Phys. 91 (2005) 40-46.
6. S.G. Huang, J. the European Ceramic Society 27 (2007) 3269-3275.
7. http://en.wikipedia.org/wiki/Elastic properties of the elements (data page).
8. S. Paris, E. Gaffet, F. Bernard and Z.A. Munir, Scripta Materialia. 50 (2004) 691-696.
9. J. Karch, R. Birringer and H. Gleiter, Nature 330 (1987) 556-558.
10. A.M. George, J. Iniguez and L. Bellaiche, Nature 413 (2001) 54-57.
11. D. Hreniak and W. Strek, Journal of Alloys and Compounds 341 (2002) 183-186.
12. C. Xu, J. Tamaki, N. Miura and N. Yamazoe, Sensors and Actuators B: Chemical. 3 (1991) 147-155.
13. D.G. Lamas, A. Caneiro, D. Niebieskikwiat, R.D. Sanchez. D. Garcia and B. Alascio, Journal of Magnetism and Magnetic Materials 241 (2002) 207-213.
14. C.W. Nahm, C.J. Kim, Y.J. Park, B.J. Lee and B.W. Park, Electron. Mater. Lett. 4 (2008) 5-8.
15. E.S. Ahn, N.J. Gleason, A. Nakahira and J.Y. Ying, Nano Letters 1 (2001) 149-153.
16. Z. Fang and J.W. Eason, International Journal of Refractory Metals and Hard Materials 13 (1995) 297-303.
17. A.I.Y. Tok, L.H. Luo and F.Y.C. Boey, Materials Science and Engineering: A 383 (2004) 229-234.
18. H.C. Kim, I.J. shon, I.K. Jeong, I.Y. Ko, J.K. Yoon and J.M. Doh, Metals and Materials International 13 (2007) 39-45.
19. C. Suryanarayana and M. Grant Norton, X-ray Diffraction A Practical Approach, Plenum Press, P.213, New York (1998).
20. O. Knake, O. Kubaschewski and K. Hesselmann, in "Thermochemical Properties of Inorganic Substances" (Springer-Verlag press 1991).
21. R.L. Coble, J. Appl. Phys. 41 (1970) 4798-4807.
22. G. Skandan, H. Hahn, B.H. Kear, M. Roddy and W.R. Cannon, Mater. Lett. 20 (1994) 305-309.
23. Z. Shen, M. Johnsson, Z. Zhao and M. Nygren, J. Am. Ceram. Soc. 85 (2002) 1921-1927.
24. J.E. Garay, U. Anselmi-Tamburini, Z.A. Munir, S.C. Glade and P. Asoka- Kumar, Appl. Phys. Lett. 85 (2004) 573-575.
25. J.R. Friedman and J.E. Garay. U. Intermetallics. 12 (2004) 589-597.
26. J.E. Garay, J.E. Garay. U. Anselmi-Tamburini and Z.A. Munir, Acta Mater., 51 (2003) 4487-4495
27. G.R. Anstis, P. Chantikul, B.R. Lawn and D.B. Marshall, J. Am. Ceram. Soc. 64 (1981) 533-538.
28. S.G. Huang, K. Vanmeensel, O. Van der Biest and J. Vleugels, Journal of the European Ceramics Society 27 (2007) 3269-3275.